Composites: Part A 189 (2025) 108594

Contents lists available at ScienceDirect

Composites Part A

journal homepage: www.elsevier.com/locate/compositesa

COD and CSD based model for in-plane stiffness of symmetric laminates with cracks in plies and local delaminations: Analysis of crack face sliding

Janis Varna [a,b], Rodrigo T.S. Freire [c,d], Mohamed Sahbi Loukil [e,*], Nawres J. Al-Ramahi [a]

[a] Department of Engineering Sciences and Mathematics, Luleå University of Technology, Luleå, Sweden
[b] Laboratory of Experimental Mechanics of Materials, Riga Technical University, Riga, Latvia
[c] Centre for Innovation and Technology in Composite Materials, Department of Mechanical Engineering, Federal University of São João del Rei (UFSJ), 36307-344, Brazil
[d] Department of Natural Sciences, Federal University of São João del Rei (UFSJ), Brazil
[e] Department of Management and Engineering, Linköping University, Sweden

GRAPHICAL ABSTRACT

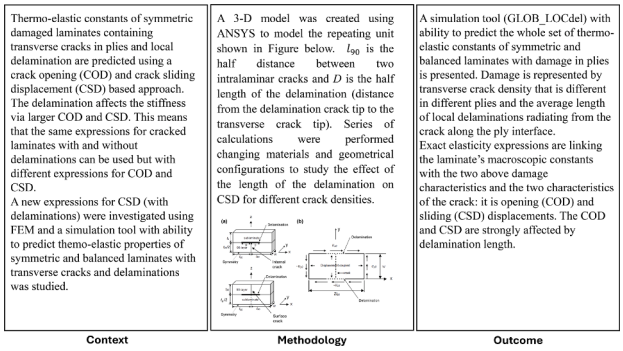

ARTICLE INFO

Keywords:
Laminates
Transverse cracks
Local delaminations
Thermo-elastic constants
Crack face displacements

ABSTRACT

In-plane thermo-elastic constants of symmetric damaged laminates containing transverse cracks in plies and local delaminations starting from crack tip are predicted using a crack opening (COD) and crack sliding displacement (CSD) based approach. An exact elastic analysis shows that the displacement gap on the delamination crack surfaces does not enter the stiffness expressions explicitly. The delamination affects the stiffness via larger COD and CSD of the intralaminar crack. This means that the same expressions for cracked laminates with and without delaminations can be used but with different expressions for COD and CSD. Finite element method is used to analyze the CSD dependence on delamination length and crack density. The obtained approximative expressions for CSD are in a good agreement with FEM. It is shown that in cases when it depends on CSD only, the predicted shear modulus of laminates is in an excellent agreement with direct FEM calculations. The used homogenization over couples of off-axis plies (monoclinic materials) in CSD expressions for balanced laminates is validated.

* Corresponding author.
E-mail address: mohamed.loukil@liu.se (M.S. Loukil).

https://doi.org/10.1016/j.compositesa.2024.108594
Received 22 August 2024; Received in revised form 12 November 2024; Accepted 13 November 2024
Available online 16 November 2024

1. Introduction

Structural elements may consist of laminates with ply (unidirectional (UD) composites) orientation selected to meet design specifications regarding service loads and environmental conditions. Microdamage appears in plies and between plies long before the macroscale failure of the laminate, affecting the load sharing between plies and changing thermo-elastic constants of the laminate.

The first mode of microdamage [1–3] is called "intralaminar cracking". The cracks are often called matrix cracks, tunneling cracks or transverse cracks. Transverse cracks, see Fig. 1a, run along fibers in the ply and usually the crack is well defined, the crack plane being perpendicular to the laminate midplane. The crack covers the whole thickness of the ply and, excepting extremely thin plies and fatigue loads, it propagates over the whole width of the tensile specimen. The transverse crack propagation is in a mixed mode, and usually Mode I energy release rate (ERR) is the most important in propagation criteria.

The effect of each individual transverse crack on laminate stiffness is very small. When the number of cracks increases, they may significantly change the thermo-elastic constants of the laminate [2,4] also initiating other damage modes, such as local delaminations starting at the intralaminar crack tip [5,6] and fiber breaks in adjacent layers, Fig. 1b, 1c and Fig. 1d. Since local delaminations are connected with the transverse crack they can be treated as a part of the same damage entity. Thus, the entity is the transverse crack with local delaminations.

The damage state in a ply is described by an averaged metric called crack density, which is defined as the number of cracks per unit distance measured in direction perpendicular to the crack plane. The stress state is different in different plies and so is the crack density. The crack density in k-th layer, denoted ρ_k, is inverse to the average distance between cracks, called an average crack spacing

$$2l_k = 1/\rho_k. \tag{1}$$

Since stiffness depends on the ratio of geometrical parameters (not on real dimensions) "normalized spacing" $2l_{kn}$ and "normalized crack density" ρ_{kn} are introduced dividing the spacing by ply thickness t_k.

$$2l_{kn} = \frac{2l_k}{t_k},\ \rho_{kn} = t_k/2l_k = \rho_k t_k, \tag{2}$$

The delamination length D_k is the distance from the delamination crack tip to the transverse crack, see Fig. 1d. It is also normalized with respect to the cracked ply thickness, $D_{kn} = D_k/t_k$.

Laminates with the same ply thickness ratio, normalized crack density and normalized delamination length have identical stiffness.

The two surfaces of a transverse crack are traction free if the crack is open: the in-plane transverse and shear stresses on the crack surface are zero. With increasing distance from the crack these stresses recover. The rest of plies in this region are overloaded which is the cause of laminate stiffness change. The stress transfer from the undamaged ply to the damaged is through out-of-plane shear stresses; shear-lag models approximately describe it, for example. The normalized distance needed to recover most of the Classical laminate theory (CLT) stress state depends on the stiffness and thickness ratios of the damaged and the adjacent plies and on the normalized delamination length. It has been shown [7] that the average value of the in-plane stress perturbation in the ply defines the amount of stiffness change caused by a crack.

Analytical and/or numerical methods have been used to calculate the stress state in the cracked ply of a laminate containing homogenized plies. In this so called "micromechanics modelling", the focus is on the local stress state determination between two cracks. The simplest approximate solutions are based on shear lag assumptions or on variational principles [8–14] Unfortunately, most of the analytical solutions are applicable to cross-ply type of laminates only and the accuracy is rather low. Higher accuracy requires more complex models, and the calculation codes become increasingly complex [15,16]. Only some of the semi-analytical models are generalized for cracks with delaminations [6,17–23]. The most common, [6,19], is the assumption that it is sufficient to analyze the stress in the bonded region only, erroneously assuming that the stress is zero in the whole delaminated zone of the damaged ply. The stress field models in [19,21] are using 2D shear lag assumptions. Whereas in [19] a linear dependence of out-of-plane stresses on the thickness coordinate is assumed, in [21] the thickness dependence of displacements is assumed parabolic in the undamaged plies and described with a power function in damaged plies making it more accurate. The selection of the exponent in the power function term is unclear, claiming that they do not depend on the laminate lay-up and elastic constants. In [22] the stress field in laminates with cracks and delaminations in several layers of the same orientation is found using the principle of minimum complementary energy with dividing plies in several very thin sublayers reaching similar accuracy as with fine FEM mesh.

In [6,20,23] the stress fields, calculated by the models in [6,21,23] are used to calculate energy release rate due to delamination growth and predictions are made. In [23] it is done for cyclic loading, predicting the crack density growth and the delamination growth simultaneously. The cited papers are limited to laminates with one system of cracks but suggestion for dealing with multiple systems is given in [19] using the so called "Equivalent Constraint Approach" which basically means that analyzing the stress state in one damaged layer the rest of the damaged plies is homogenized and their effective stiffness is used, leading to iterative procedure.

Alternative descriptors reflecting the average in-plane stress change are averages of the opening and sliding displacements of the crack faces

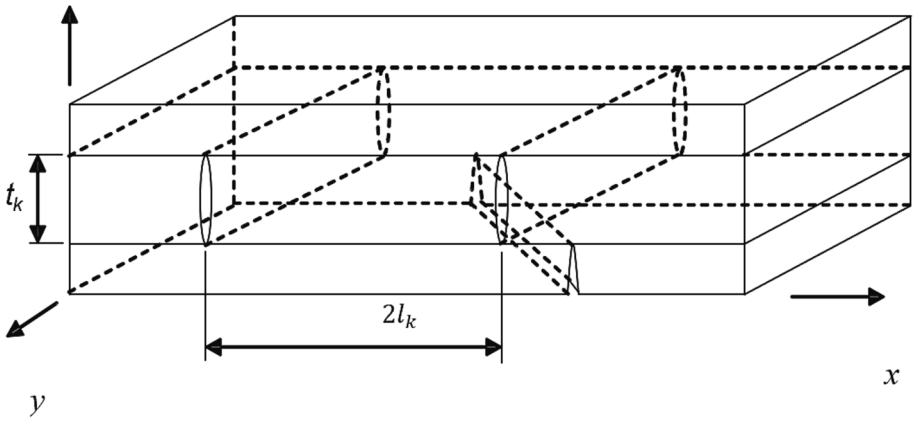

Fig. 1a. Intralaminar cracks without delamination in the model for symmetric laminates, Upper part of a symmetric laminate with cracks in layers, index 2 for displacement denotes the x-direction, index 1 the y-direction.

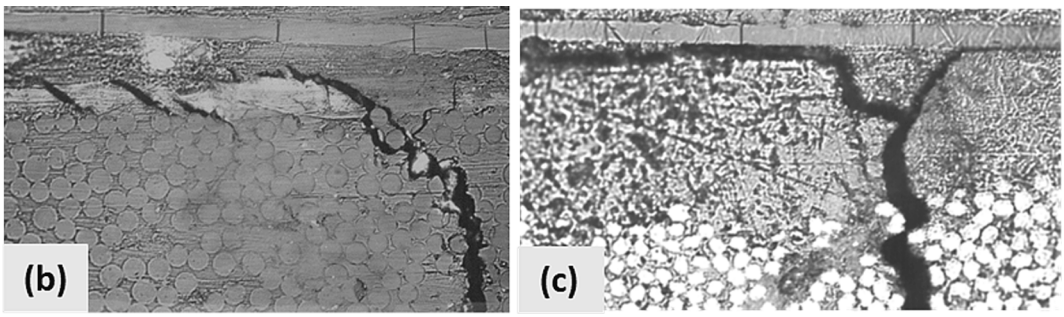

Fig. 1b, c. Initiation of a delamination from the transverse crack tip; c) growth of the local delamination along the interface.

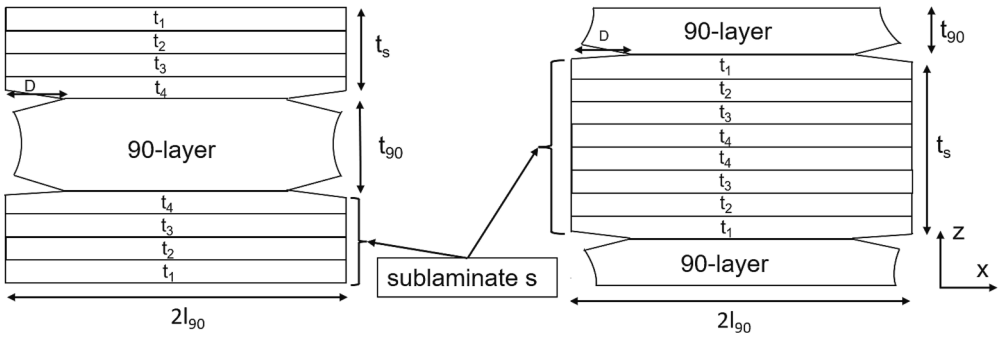

Fig. 1d. Models of the deformed repeating element between two cracks. For better visualization, the delamination crack is shown as open.

(COD and CSD). It was shown [7] that COD and CSD are proportional to the average of in-plane stress perturbations in the damaged ply. The use of COD and CSD for laminate stiffness predictions was first suggested in [24,25] for the case with zero delaminations.

[1,26,27] presented a similar approach in the framework of the CLT. The formulation (called GLOB-LOC approach) follows the same procedure as developing the CLT. Exact expressions for in-plane stiffness matrix, compliance matrix and thermal expansion coefficients of an arbitrary symmetric laminate with a different number of cracks in different plies are presented. These relationships contain thermo-elastic constants of the UD composite, geometrical characteristics of the lay-up, crack density for all plies and two very robust parameters of the crack: the average crack face opening (COD) and the average sliding displacement (CSD) normalized with respect to the CLT stress in the ply corresponding to the applied stress. In [27–32] the normalized COD and CSD were analyzed using FEM formulating approximate fitting functions. The obtained COD and CSD expressions do not account for possible interactions between cracks in different layers.

Delaminations linked with the transverse crack increase the COD and CSD of this crack. The most extreme case is a fully delaminated unit between two cracks resulting in zero in-plane stresses in the cracked ply. This case, which is called "the ply-discount model", corresponds to the maximum possible values of COD and CSD.

In this paper, the COD and CSD based approach (called GLOB-LOCdel) is generalized for in-plane thermo-elastic constant calculations of laminates with intralaminar cracks and local delaminations. The laminates and the damage state have a symmetry with respect to middle-plane. Thus, the objectives of the present paper are:

a) to generalize COD and CSD based approach for the case with local delaminations (to be called GLOB-LOCdel);

b) to perform FEM analysis of the normalized average CSD dependence on the laminate lay-up, ply properties, crack density and delamination length, establishing simple fitting functions. The COD depends on more parameters than CSD and, therefore, its analysis and development of fitting functions is left for a separate paper. For example, the stress state of $[S_n/90_8]_s$ *laminate in shear and the CSD depend on ratios* $\frac{G^s_{xy}}{G_{LT}}$, $\frac{G^s_{yz}}{G_{LT}}$, $\frac{t_s}{t_{90}}$ *only. Upper index s is used to denote the homogenized adjacent sublaminate consisting of plies of different orientations,* G_{LT} *is the in-plane shear modulus of the UD 90-ply,*

c) to use the GLOB-LOCdel and the fitting functions for CSD, analyzing shear modulus of general laminates and comparing with FEM.

It has to be emphasized that while cracks with delaminations have a distinct effect on in-plane stiffness, the largest effect is on out-of-plane thermo-elastic properties of laminates (out-of-plane shear and normal modulus) not covered in the presented paper.

2. General theory

2.1. Stress–strain response of laminates with ply cracks and delaminations

In this section we will present methodology for calculation of in-plane thermo-elastic constants of symmetric laminates with cracks in plies. The upper half of the considered symmetric *N*- ply laminate is shown in Fig. 1a. The *k*-th ply of the laminate has thickness t_k and the fiber orientation angle is θ_k. Direction "L" is the local fiber direction in the ply and direction "T" is transverse to fibers (called also 1 and 2 directions). The thickness of the laminate, $h = \sum_{k=1}^{N} t_k$. Each ply may contain a number of intralaminar cracks that is quantified by crack density in the ply ρ_k or by the dimensionless crack density ρ_{kn}, see (1) and (2). Together with the normalized delamination length, $D_{kn} = D_k/t_k$, see Fig. 1b, they are parameters characterizing the damage state. We assume that the number of cracks is the same in two plies symmetrically located with respect to the midplane. "Vector" (column of three elements) and 3×3 matrix objects are in the following denoted by {} and [] respectively. A bar above the matrix and vector entities indicates thermo-elastic constants of a ply and stress/strain in the ply in the global coordinate system x,y.

For an **undamaged** laminate the macroscopic elastic stress–strain relationship in global coordinates, expressed through stiffness matrix $[Q]_0^{LAM}$ and thermal expansion coefficient vector $\{\alpha\}_0^{LAM}$ is

$$\{\sigma\}_0^{LAM} = [Q]_0^{LAM}\left(\{\varepsilon\}_0^{LAM} - \{\alpha\}_0^{LAM}\Delta T\right) \tag{3}$$

The undamaged laminate stiffness in CLT is calculated as

$$[Q]_0^{LAM} = \frac{1}{h}\sum_{k=1}^{N}[\overline{Q}]_k t_k \tag{4}$$

Thermal expansion coefficients $\{\alpha\}_0^{LAM}$ are determined solving the thermal CLT problem

$$\frac{1}{h}\{N\}^{th} = [Q]_0^{LAM}\{\alpha\}_0^{LAM}\Delta T, \text{where } \{N\}^{th} = \Delta T\sum_{k=1}^{N}[\overline{Q}]_k\{\overline{\alpha}\}_k t_k, \{\overline{\alpha}\}_k = [T]_k^T\begin{Bmatrix}\alpha_L\\ \alpha_T\\ 0\end{Bmatrix}, \tag{5}$$

In **(5)** $[T]_k^T$ is the transposed stress transformation matrix between local and global coordinates for ply with fiber orientation angle θ_k. The undamaged laminate compliance matrix is $[S]_0^{LAM} = \left([Q]_0^{LAM}\right)^{-1}$.

The stress–strain relationship for **damaged** laminate can be written as

$$\{\sigma\}_0^{LAM} = [Q]^{LAM}\left(\{\varepsilon\}^{LAM} - \{\alpha\}^{LAM}\Delta T\right) \tag{6}$$

In the damaged laminate, the stiffness matrix is different and the same applied stress as for the undamaged laminate will cause a different strain response. The damaged laminate has a stiffness matrix $[Q]^{LAM}$ and a vector of thermal expansion coefficients $\{\alpha\}^{LAM}$. The objective is to derive expressions for them that will depend on UD thermo-elastic constants, the laminate lay-up, on the crack densities, COD, CSD and delamination length in plies.

Derivation of constitutive equations for the damaged laminate with delaminations follows the same path as for damaged laminates without delaminations [1,27]. The stresses averaged over the whole laminate volume $V = hS$ and the strains averaged in each ply with volume $V_k = St_k$ (S is the in-plane surface area of the RVE) are defined as

$$\{\sigma\}^{(av)} = \frac{1}{V}\iiint_V\{\overline{\sigma}\}dv,\ \ \{\overline{\varepsilon}\}_k^{(av)} = \frac{1}{St_k}\iiint_{V_k}\{\overline{\varepsilon}\}_k dv \tag{7}$$

From the divergence theorem follows, see [33] that the macroscopic stress applied to the laminate RVE boundary is equal to the volume averaged stress

$$\{\sigma\}_0^{LAM} = \{\sigma\}^{(av)}, \tag{8}$$

An integral over the laminate volume can be written as a sum of integrals over volumes of all plies, leading to

$$\{\sigma\}_0^{LAM} = \sum_{k=1}^{N}\frac{t_k}{h}\{\overline{\sigma}\}_k^{(av)} \tag{9}$$

The Hook's law for the volume averaged stresses in a ply has the same form as it is in each point

$$\{\overline{\sigma}\}_k^{(av)} = [\overline{Q}]_k\left(\{\overline{\varepsilon}\}_k^{(av)} - \{\overline{\alpha}\}_k\Delta T\right) \tag{10}$$

Using the divergence theorem the average strain in the damaged ply, $\{\overline{\varepsilon}\}_k^{(av)}$ entering (10) can be expressed through the external boundary averaged strains (applied laminate strain $\{\varepsilon\}^{LAM}$) and the averaged displacements on crack surfaces, see [34] for details

$$\{\overline{\varepsilon}\}_k^{(av)} = \{\varepsilon\}^{LAM} + \{\overline{\beta}\}_k \tag{11}$$

In (11) $\{\overline{\beta}\}_k$ is the Voigt's vectorial representation of the Vakulenko-Kachanov tensor

$$\overline{\beta}_{ij}^k = \frac{1}{V_k}\int_{S_c}\frac{1}{2}\left(u_i^k n_j + u_j^k n_i\right)dS, \qquad i,j = x,y \tag{12}$$

$$\{\overline{\beta}\}_k = \begin{Bmatrix}\overline{\beta}_{xx}\\ \overline{\beta}_{yy}\\ 2\overline{\beta}_{xy}\end{Bmatrix}_k \tag{13}$$

Integration in (12) is over S_C which is the total surface of all cracks in the layer, u_i are displacements of the points on the crack surface, n_j are components of the outer normal to the crack face.

Substituting (11) in (10) and using the result in (9) we obtain

$$\{\sigma\}_0^{LAM} = [Q]_0^{LAM}\{\varepsilon\}^{LAM} - \sum_{k=1}^{N}\frac{t_k}{h}[\overline{Q}]_k\{\overline{\alpha}\}_k\Delta T + \sum_{k=1}^{N}\frac{t_k}{h}[\overline{Q}]_k\{\overline{\beta}\}_k \tag{14}$$

The CLT expression (4) was used obtaining (14). The second term in (14) is the "thermal force" $\{N\}^{th}$ divided by laminate thickness (see definition (5)) which can be expressed through thermal expansion coefficients of the undamaged laminate. This procedure results in

$$\{\sigma\}_0^{LAM} = [Q]_0^{LAM}\left(\{\varepsilon\}^{LAM} - \{\alpha\}_0^{LAM}\Delta T\right) + \sum_{k=1}^{N}\frac{t_k}{h}[\overline{Q}]_k\{\overline{\beta}\}_k \tag{15}$$

The last term in (15) represents the effect of the two components of the crack face displacement (opening and sliding) on the laminate stiffness that is analyzed in the next section.

2.2. Displacements on the face of delamination crack and intralaminar crack

The elements of the Vakuleno-Kachanow tensor (12) for the k-th ply are analyzed here in local coordinates of the ply where indexes 1, 2 and 3 correspond to the longitudinal (L), transverse (T) and thickness (z) directions.

Transformation between local and global coordinates for Vakulenko-Kachanov tensor β_{ij} is given by

$$\{\overline{\beta}\}_k = [T]_k^T\begin{Bmatrix}\beta_{11}\\ \beta_{22}\\ 2\beta_{12}\end{Bmatrix}_k \tag{16}$$

Since the β_{ij} has the meaning of additional strain its transformation expression is the same as for in-plane strains. To find the meaning of $\{\beta\}_k$ elements we use definition (12), separately analyzing displacements on the surfaces of the delamination crack and the transverse crack. Each crack has two faces with opposite directions of the outer normal to the face

A. The delamination crack has orientation of the normal vector $n_1 = n_2 = 0$, $n_3 = \mp 1$. Hence, from (12) follows that the delamination crack's displacements are not contributing to $\{\beta\}_k$. However, they strongly affect the displacements of the faces of the transverse crack. It must be noted that displacements of delamination cracks would directly affect β_{i3} and the out-of-plane elastic constants of the laminate not analyzed in this paper.
B. The transverse crack has the following outer normal vector to the two faces

$$n_1 = n_3 = 0, n_2^+ = -1, n_2^- = +1, \tag{17}$$

"+" and "-" denote the "right" and "left" crack face in Fig. 1e.

Using (12) for β_{ij}^k in the k-th ply of volume $V_k = Lwt_k$, with one crack face surface area equal to wt_k and with R cracks inside the ply (w is the width of the specimen), we see that $\beta_{11}^k = 0$ and the tensor contains only two non-zero in-plane elements: β_{12}^k and β_{22}^k

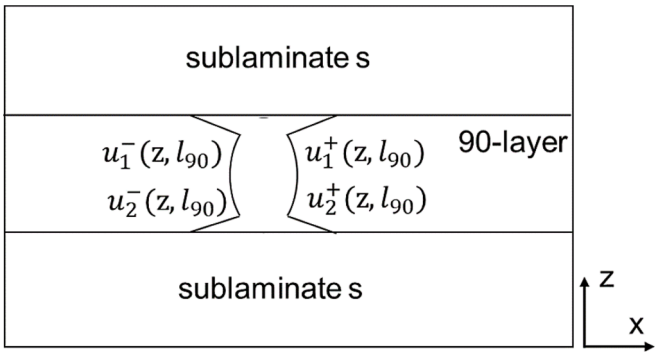

Fig. 1e. Notation used for displacements of crack faces.

$$\beta_{12}^k = \frac{w}{Lwt_k}\sum_{r=1}^{R}\int_{-\frac{t_k}{2}}^{+\frac{t_k}{2}}\frac{1}{2}\left[-u_{1(r)}^{k+}(z)+u_{1(r)}^{k-}(z)\right]dz \tag{18}$$

$$\beta_{22}^k = \frac{w}{Lwt_k}\sum_{r=1}^{R}\int_{-\frac{t_k}{2}}^{+\frac{t_k}{2}}\left[-u_{2(r)}^{k+}(z)+u_{2(r)}^{k-}(z)\right]dz \tag{19}$$

The two terms under the sign of the integral in (18), (19) correspond to the two surfaces of the crack. They may be different and not the same for all cracks if the crack distribution is non-uniform. Assuming equal cracks and uniform crack distribution, $u_{1(r)}^{k-} = -u_{1(r)}^{k+} = -u_1^{k+}, u_{2(r)}^{k-} = -u_{2(r)}^{k+} = -u_2^{k+}$,

$$\beta_{12}^k = \frac{-R}{Lt_k}\int_{-\frac{t_k}{2}}^{+\frac{t_k}{2}}\left[u_1^{k+}(z)\right]dz,\ \beta_{22}^k = \frac{-2R}{Lt_k}\int_{-\frac{t_k}{2}}^{+\frac{t_k}{2}}\left[u_2^{k+}(z)\right]dz \tag{20}$$

Using the definition of the crack density (1) and (22)

$$\beta_{12}^k = -\rho_k u_{1a}^k,\ \beta_{22}^k = -2\rho_k u_{2a}^k \tag{21}$$

In (21), u_{1a}^k and u_{2a}^k are averaged (index a) transverse crack face sliding (in L- direction) and opening (in T-direction) displacements defined as

$$u_{2a}^k = \frac{1}{t_k}\int_{-\frac{t_k}{2}}^{+\frac{t_k}{2}} u_2^k(z)dz,\ u_{1a}^k = \frac{1}{t_k}\int_{-\frac{t_k}{2}}^{+\frac{t_k}{2}} u_1^k(z)dz \tag{22}$$

In (22) u_2^k, u_1^k is the distance in transverse and longitudinal direction respectively between corresponding points on the deformed crack surface and the crack plane (the surface connecting both crack tips). The crack density in (21) can be replaced with the normalized crack density ρ_{kn} using (2) and the average COD and CSD may be replaced with the normalized values u_{2an}^k and u_{1an}^k defined as

$$u_{2an}^k = \frac{u_{2a}^k}{\sigma_{T0}^{(k)}t_k}E_T,\ u_{1an}^k = \frac{u_{1a}^k}{\sigma_{LT0}^{(k)}t_k}G_{LT} \tag{23}$$

In (23) $\sigma_{T0}^{(k)}$ and $\sigma_{LT0}^{(k)}$ are the in-plane local stress components in the ply of the undamaged laminate calculated using CLT at applied $\{\sigma\}_0^{LAM}$ and temperature change ΔT. The obtained expressions in local coordinates can be written in matrix form

$$\{\beta\}_k = \begin{Bmatrix}0\\ \beta_{22}\\ 2\beta_{12}\end{Bmatrix}_k = -2\frac{\rho_{kn}}{E_T}[U]_k\begin{Bmatrix}\sigma_{L0}\\ \sigma_{T0}\\ \sigma_{LT0}\end{Bmatrix}_k \tag{24}$$

$$[U]_k = \begin{bmatrix}0 & 0 & 0\\ 0 & u_{2an}^k & 0\\ 0 & 0 & \frac{E_T}{G_{LT}}u_{1an}^k\end{bmatrix} \tag{25}$$

The values of u_{1an}^k and u_{2an}^k depend on the crack density (due to interaction of stress perturbations from two adjacent cracks) and the delamination length. The found dependencies are presented in Section 4. In terms of COD and CSD of the transverse crack, the obtained expression for $\{\beta\}_k$ (24) is exactly as in the case with zero delaminations, just the COD and CSD are larger. Hence, we have shown that all expressions for damaged laminate thermo-elastic constants written in terms of u_{1an}^k and u_{2an}^k formally retain the same form as in the zero-delamination case analyzed in [28]

$$[Q]^{LAM} = \left([I]+\sum\nolimits_{k=1}^{N}\rho_{kn}\frac{t_k}{h}[K]_k[S]_0^{LAM}\right)^{-1}[Q]_0^{LAM} \tag{26}$$

$$\{\alpha\}^{LAM} = \left([I]+\sum\nolimits_{k=1}^{N}\rho_{kn}\frac{t_k}{h}[S]_0^{LAM}[K]_k\right)\{\alpha\}_0^{LAM} - \sum\nolimits_{k=1}^{N}\rho_{kn}\frac{t_k}{h}[S]_0^{LAM}[K]_k\{\overline{\alpha}\}_k \tag{27}$$

In (26),(27) $[I]$ is the identity matrix. A new matrix $[K]_k$ that shows the effect of a crack in the k-th ply is introduced.

$$[K]_k = \frac{2}{E_T}[\overline{Q}]_k[T]_k^T[U]_k[T]_k[\overline{Q}]_k \tag{28}$$

The effect of delaminations on the in-plane stiffness enters via the COD and CSD in (25) that is the critical part of $[K]_k$. They are significantly larger in the presence of large delaminations. Expressions (26) and (27) are exact formulas for in-plane thermo-elastic properties of symmetric laminates with known damage state.

2.3. Stiffness of balanced laminates with cracks in several plies with the same orientation

Any symmetric laminate can be rotated to the global coordinate system where the damaged ply becomes a 90-ply. Then, the global coordinate x, that is the axial direction of the laminate, coincides with direction 2 for the 90-ply, y is in the in-plane lateral direction and it coincides with direction 1 and z is in the thickness direction.

We may have one central 90-ply in the laminate and couples of 90-plies with a given distance from the midplane. A particular case for the latter is damaged surface 90-plies.

If in this system of coordinates the laminate is balanced (practical examples are cross-ply laminates and any quasi-isotropic laminate), the matrix operations (25)-(28) are simpler and analytical expressions for that case presented in [1,31,34,35] are repeated here.

For balanced and symmetric laminates with symmetric damage state in 90-plies

$$\frac{E_x^{LAM}}{E_{x0}^{LAM}} = \frac{1}{1+2M\rho_{90n}\frac{t_{90}}{h}u_{2an}^{90}c_2},\ \frac{E_y^{LAM}}{E_{y0}^{LAM}} = \frac{1}{1+2M\rho_{90n}\frac{t_{90}}{h}u_{2an}^{90}c_4} \tag{29}$$

$$\frac{\nu_{xy}^{LAM}}{\nu_{xy0}^{LAM}} = \frac{1+2M\rho_{90n}\frac{t_{90}}{h}u_{2an}^{90}c_1\left(1-\frac{\nu_{LT}}{\nu_{yx0}^{LAM}}\right)}{1+2M\rho_{90n}\frac{t_{90}}{h}u_{2an}^{90}c_2},\ \frac{G_{xy}^{LAM}}{G_{xy0}^{LAM}} = \frac{1}{1+2M\rho_{90n}\frac{t_{90}}{h}u_{1an}^{90}\frac{G_{LT}}{G_{xy0}^{LAM}}} \tag{30}$$

$$c_1 = \frac{E_T}{E_{x0}^{LAM}}\frac{1-\nu_{LT}\nu_{xy0}^{LAM}}{(1-\nu_{LT}\nu_{TL})^2},\ c_2 = c_1\left(1-\nu_{LT}\nu_{xy0}^{LAM}\right) \tag{31}$$

$$c_3 = \frac{E_T}{E_{y0}^{LAM}} \frac{\nu_{LT} - \nu_{yx0}^{LAM}}{(1-\nu_{LT}\nu_{TL})^2},\ c_4 = \frac{E_T}{E_{yo}^{LAM}} \frac{\left(\nu_{LT} - \nu_{yx0}^{LAM}\right)^2}{(1-\nu_{LT}\nu_{TL})^2} \tag{32}$$

The thermal expansion coefficients of the damaged laminate are

$$\frac{\alpha_x^{LAM}}{\alpha_{x0}^{LAM}} = 1 - 2M\rho_{90n}\frac{t_{90}}{h}u_{2an}^{90}\frac{c_1}{\alpha_{x0}^{LAM}}\left(\alpha_2 - \alpha_{x0}^{LAM} - \nu_{12}\left(\alpha_{y0}^{LAM} - \alpha_1\right)\right) \tag{33}$$

$$\frac{\alpha_y^{LAM}}{\alpha_{y0}^{LAM}} = 1 - 2M\rho_{90n}\frac{t_{90}}{h}u_{2an}^{90}\frac{c_3}{\alpha_{y0}^{LAM}}\left(\alpha_2 - \alpha_{x0}^{LAM} - \nu_{12}\left(\alpha_{y0}^{LAM} - \alpha_1\right)\right) \tag{34}$$

Index 90 is used for the 90-ply thickness, crack density, COD and CSD. The quantities with upper index "LAM" are laminate constants, quantities with additional lower index 0 are undamaged laminate constants. For laminates with damaged central 90-ply only, M = 1. For laminates with a couple of symmetrically located damaged 90-plies with the same crack density in both 90-plies, the contribution to laminate stiffness of both plies is the same and, therefore, terms with crack density in the ply, ρ_{90n} have to be multiplied by M = 2. These expressions will be used in Section 5 validating the developed approach.

If the number of different couples of damaged 90-plies is J, and each couple is of a different thickness, a sum over contributions of all couples $2M\sum_{j=1}^{J}\rho_{90n}^{(j)}\frac{t_{90}^{(j)}}{h}u_{2an}^{90(j)}$ has to be used in equations. In that case,u_{2an}^{90} and u_{1an}^{90} may be different in 90-plies with different thickness and location, see Section 4 and 5.

Standard stiffness transformation expressions for orthotropic materials can be used to re-calculate the calculated laminate stiffness to any other coordinates where the damaged ply has a different orientation.

It is noteworthy that for the considered type of balanced laminates the shear modulus G_{xy}^{LAM} does not depend on u_{2an}^{90}, it depends on sliding displacement only. On the other hand, the sliding displacement u_{1an}^{90} does not enter expressions for $E_x^{LAM}, E_y^{LAM}, \nu_{xy}^{LAM}$ and, therefore, calculating these constants the value of CSD is of no significance.

3. FEM modelling of CSD in 90-plies of symmetric laminates

In the performed parametric analysis, the 90-ply is transversely isotropic and $E_2 = E_3 = E_T; G_{12} = G_{13} = G_{LT}$ and $\upsilon_{12} = \upsilon_{13} = \nu_{LT}$. The lay-up of plies adjacent to the damaged 90-ply is homogenized and called "sublaminate", see Fig. 1d and Fig. 1e. Elastic constants and geometrical parameters with index "s" refer to homogenized properties of the orthotropic sublaminate.

If the crack is open $u_{2an}^{90} \neq 0$, the stress distribution in plies depends on three elastic moduli of the damaged ply, two Poisson's ratios and an even larger number of constants for an orthotropic sublaminate and on the thickness ratio t_s/t_{90}. Obviously, u_{2an}^{90} also depends on all these parameters.

On the other hand, the sliding of crack faces is caused by shear stresses in the damaged ply. In the laminate lay-up with an orthotropic sublaminate and damaged 90-ply numerically analyzed below, it is achieved applying in-plane shear load to the laminate. Hence, the stress distribution in plies and consequently also the u_{1an}^{90} depend on ratios $\frac{G_{xy}^s}{G_{LT}}$, $\frac{G_{yz}^s}{G_{LT}}$, $\frac{t_s}{t_{90}}$. In a case of cross-ply laminate $G_{xy}^s = G_{12}$ and $G_{yz}^s = G_{23}$. The rest of elastic constants $E_1, E_2 = E_3, \nu_{12}$ of the 90-ply and $E_x^s, E_y^s, E_z^s, \nu_{xy}^s, \nu_{xz}^s$ etc of the orthotropic sublaminate do not affect the stress state in shear loading.

A UD composite with $E_L = 45GPa$, $E_T = 15GPa$,$G_{LT} = 4.5GPa$ $\nu_{LT} = 0.3$ $G_{T3} = 5.36GPa$ is used as the 90-ply in FEM calculations.

Because of a smaller number of parameters in the CSD analysis than in COD analysis and due to the limited space in the paper the shear case only is presented in this paper developing expressions for u_{1an}^{90} by fitting FEM results.

Thus, symmetric laminates in a coordinate system where they are balanced and the 90-ply with cracks is in the middle or a laminate with two cracked surface plies are analyzed. Coordinate x is the axial direction coinciding with the T-direction of the 90-ply, y is in the in-plane lateral direction coinciding with L-direction and z is in the thickness direction. Laminates with lay-up $[S_n/90_8]_s$ and $[90_8/S_n]_s$ with orthotropic sublaminates are used in analysis. In the first laminate, the 90-ply thickness is $t_{90} = 2 \bullet 8 = 16$, the sublaminate thickness takes values $t_s = n$ and the laminate thickness is $h = t_{90} + 2t_s$ In the second laminate, $t_{90} = 8, t_s = 2 \bullet n$ and the laminate thickness is $h = 2t_{90} + t_s$. Parameter $n = 4, 8, 16$.

3.1. Methodology

The commercial code ANSYS 19 was used in FEM calculations. In the model, the intralaminar cracks are uniformly distributed and delaminations are symmetric with respect to the intralaminar crack plane. A 3-D model was created to model the repeating unit shown in Fig. 2. l_{90} is the half distance between two intralaminar cracks and D is the half length of the delamination (distance from the delamination crack tip to the transverse crack tip).

Series of calculations were performed changing materials and geometrical configurations to study the effect of the length of the delamination on CSD for different crack densities. The displacement in y-direction for the nodes on the intralaminar crack surface was used to calculate the value of the CSD. The obtained CSD was averaged according to (22) and normalized according to (23).

Studying the normalized average crack sliding displacement dependence on the length of the delamination, the delamination length D was varied from 0 to 0.9 $*l_{90}$ (from zero delamination to almost fully delaminated 90-ply). The total number of simulations was about 500.

3.2. Element type, boundary conditions and mesh

Default SOLID186 elements were used. The 3D model contains the upper half of the RVE with one crack in the 90-ply, applying symmetry on the surface $z = 0$, see Fig. 2a. The top surface $z = \frac{h}{2}$ is traction-free. Tangential displacements are applied to the side surfaces (edges), see Fig. 2b. The relationship $\frac{U_{y0}}{2l_{90}} = \frac{U_{x0}}{W}$ and coupling of the rest of displacement components to ensure independence of solution on the y-coordinate were applied as described below. Each point on the surface at $y = w$ has the same displacement in z and y-direction as the corresponding point on the surface at $y = 0$. In the same way the points on the surfaces at $x = -l_{90}$ and $x = l_{90}$ have the same displacement in z and x direction. Thus, we are not simulating a specimen but an RVE. These periodicity conditions are sufficient for macroscopically orthotropic laminates only. Tangential force was calculated and from there the laminate-scale shear stress was found. The result of calculations is the dependence of the average normalized CSD and the laminate shear modulus on the normalized crack density, delamination length, geometrical and elastic parameters.

Three elements in the width direction and small width of the FEM model were used, which is more than sufficient for stress states that do not depend on y-coordinate. A refined mesh was used near to the damaged region. Depending on the crack density and on the delamination length, the number of elements was increased with the line length, and it was finer closer to the crack tip. There was never a problem with element aspect ratio because the selected width of the model was small. A convergence study was performed to ensure accuracy of results. Surface to surface contact elements (CONTA 174) in the 90-ply delaminated zone, were paired to target elements (TARGE 170) in the 0-ply delaminated region.

4. Approximation functions for CSD

Since only one ply is damaged (90-ply in the used coordinate system)

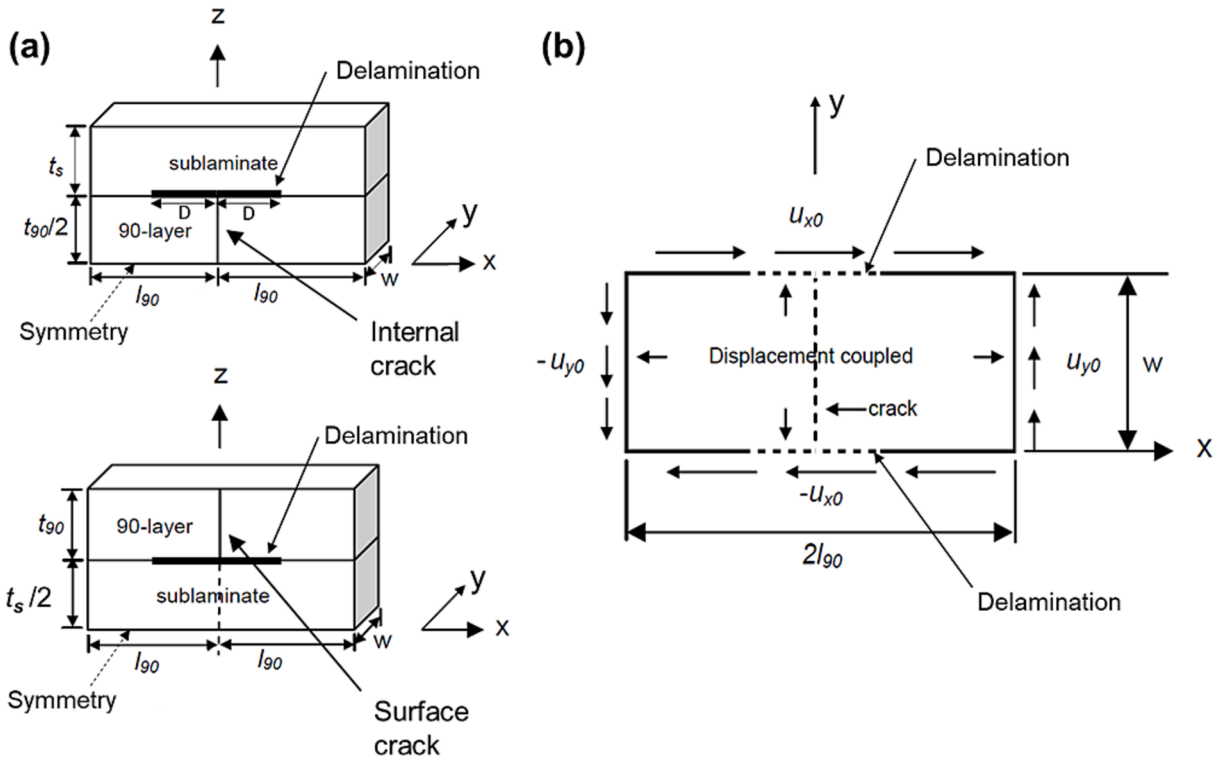

Fig. 2. The FEM model: (a) upper part of the symmetric models used for calculation of sliding displacements (b) applied boundary conditions used for pure shear modeling.

index k for the damaged ply in (22), (23) is omitted in following. As a result of FEM analysis of CSD in cases with delamination length $D_n = 0$, [1,24,29,32], approximate expressions for $u_{1an}(D_n = 0)$ where obtained. The fitting constants in expressions slightly differ in different papers but the calculated values u_{1an} are very similar. In the current paper we use following expressions

$$u_{1an}(D_n = 0) = u^0_{1an}\varphi(\rho_n) \tag{35}$$

In (35), u^0_{1an} is the CSD of a non-interactive crack ($\rho_n \to 0$)

$$u^0_{1an} = K\left[0.31 + (0.066 + 0.054 \bullet 2F)\left(\frac{G^s_{xy}}{G_{12}}\right)^{-0.82}\right] \tag{36}$$

In (36), $K = 1$ for inside plies and $K = 2$ for surface plies, F is geometrical parameter with a different definition for inside- and surface plies, see Fig. 1d

$$F = \begin{cases} \dfrac{t_{90}}{(4t_s)} \textit{ in internal plies} \\ \dfrac{t_{90}}{t_s} \textit{ in surface plies} \end{cases} \tag{37}$$

The interaction function$\varphi(\rho_n) < 1$, which describes the lowering of CSD due to interaction with neighboring crack in the same ply, is modified to account for the effect of the delamination length

$$\varphi(\rho_n, D_n) = \tanh\left[\frac{\mu}{K}\left(\frac{1}{\rho_n} - 2D_n\right)\right], \mu = \sqrt{3\frac{1 + K_1\frac{G_{LT}}{G^s_{xy}}}{1 + 3\frac{G_{LT}}{G^s_{yz}}K_2}} \tag{38}$$

In [32], K_1 and K_2 were defined as

$$K_1 = \frac{d}{z_1},\ K_2 = \frac{z_1}{3d} \tag{39}$$

where $d = t_{90}/2$ for $[S_n/90_8]_s$ laminate and $d = t_{90}$ for $[90_8/S_n]_s$ laminate, z_1 is the size of the shear stress perturbation zone inside the sublaminate S in thickness direction with approximate values given in section 5.1.

The fitting expressions (40)-(47) below were found by tedious numerical data analysis. Their applicability is limited by the range of parameters used in the parametric analysis.

($\frac{t_{90}}{h} > 0.25; 4 > \frac{G^s_{xy}}{G_{12}} > 0.5$) and using them outside this range can introduce errors.

Section 5 illustrates their applicability and accuracy.

In the region $\frac{1}{K}\left(\frac{1}{\rho_n} - 2D_n\right) \geq 1$ and $D_n \leq 2$, the $u_{1an}(\rho_n, D_n)$ is fitted with a second order polynomial

$$u_{1an} = u^0_{1an}\varphi(\rho_n, D_n)\left[1 + R_1\frac{D_n}{K} + R_2\left(\frac{D_n}{K}\right)^2\right] \tag{40}$$

Expressions for R_1 and R_2 are

$$R_1 = 2.1 + 4.0\left(\frac{G_{LT}}{G^s_{xy}}F\right)^{0.5} \tag{41}$$

$$R_2 = -1.45\left(\frac{G_{LT}}{G^s_{xy}}\right)^{0.5} F^{0.7} \tag{42}$$

For very short, bonded regions between tips of delamination cracks (highly interactive cracks) where $0.4 < \frac{1}{M}\left(\frac{1}{\rho_n} - 2D_n\right) \leq 1$

$$u_{1an} = u^0_{1an}\tanh\mu \bullet \left[1 + R_1\frac{D_n}{2} + R_2\left(\frac{D_n}{2}\right)^4\right] \tag{43}$$

In the considered region R_1 and R_2 expressions for internal and surface plies are different.

For internal 90-ply

$$R_1 = 6.4 + 5 \bullet \left(\frac{G_{LT}}{G^s_{xy}}\right)^{0.8} F^{0.65} \quad (44)$$

$$R_2 = -22 \bullet \left(\frac{G_{LT}}{G^s_{xy}}\right)^{0.15} \quad (45)$$

For surface 90-ply:

$$R_1 = 2.1 + 3.3 \bullet \left(\frac{G_{LT}}{G^s_{xy}}\right)^{0.8} F^{0.65} \quad (46)$$

$$R_2 = -12 \bullet \left(\frac{G_{LT}}{G^s_{xy}}\right)^{0.4} \quad (47)$$

5. Examples of accuracy of u_{1an} expressions and laminate shear modulus predictions

In this section, expressions presented in section 4 are used to compare calculation for u_{1an} and for the laminate shear modulus with FEM using damage states with two values of $\rho_n = 0.1$ and 0.5 and a wide range of delaminatation length D_n. In the noninteractive crack case ($\rho_n = 0.1$), the delamination length reaches $2t_{90}$, in the most interactive crack case ($\rho_n = 0.5$) and $D_n = 0.9$ corresponds to 90 % of the interface between cracks is delaminated. In figures, notation "ron" is used for ρ_n.

The elastic constants of the sublaminate are presented as ratios with respect to G_{LT}. Since all parameters in stiffness expressions, including the u_{1an}, are normalized with respect to G_{LT}, the selected G_{LT} value does not affect the calculated u_{1an}.

The out-of-plane shear modulus of a UD ply in x,y,z − coordinates depends on the ply orientation angle θ according to

$$G_{yz} = G_{23}\cos^2\theta + G_{12}\sin^2\theta \quad (48)$$

Since G_{23} and G_{12} values are in the same range, the G_{yz} of a ply is also in the same range. From here follows that the out-of-plane shear modulus G^s_{yz} of a sublaminate consisting of layers of different orientations is also in the same range. FEM calculations show that changing $G_{23} = 5.36GPa$ by 20 % up or down leads to less than 1 % change of u_{1an}. Therefore, the value of the out-of-plane shear modulus of the 90-ply and of the sublaminate is not used as a parameter.

Function $\varphi(\rho_n, D_n)$ in (38) characterizes the effect of the closeness of the adjacent crack in the same ply on the CSD of the crack under consideration. According to (38), (39), the level of interaction for cracks with zero delamination depends on parameter z_1/d which was found in [36], minimizing the complementary energy to find the best value under assumption that the out-of-plane shear stress in the stress perturbation zone in the adjacent ply is a linear function of the distance from the crack tip in the thickness direction. The estimated values for analyzed laminates are given in Table 1.

5.1. Effect of sublaminate shear modulus: $[\boldsymbol{S}_4/90_8]_s$ and $[90_8/\boldsymbol{S}_4]_s$ laminate

In this section, the effect of the sublaminte shear moduli G^s_{xy} on u_{1an} is analyzed. Parameter $k = G^s_{xy}/G_{LT}$ values $k = 0.5, 1, 2, 4, 6$ are used to compare u_{1an} in $[S_4/90_8]_s$ and $[90_8/S_4]_s$ laminates using FEM data and expressions in section 4. Value $k = 1$ corresponds to cross-ply laminate, values $k = 2, 4, 6$ could be for sublaminates containing $[\pm\theta]s$ plies with $\theta \approx 30 - 45^\circ$. The case with $k = 0.5$ is less realistic but could become relevant for hybrid laminates with plies of different materials.

In Fig. 3 u_{1an} results for noninteractive crack density $\rho_n = 0.1$ and for crack density $\rho_n = 0.5$ are presented for $[S_4/90_8]_s$ laminate. Values from FEM calculations (symbols) are shown together with calculations using equations in section 4. The u_{1an} dependence on delamination length D_n is strongly affected by $k = G^s_{xy}/G_{LT}$ the CSD becoming much smaller for large k. The accuracy of the analytical fitting expressions is excellent over the whole range of parameters, except some deviations in the case with unrealistically low $k = 0.5$ at large crack density and almost totally delaminated interface.

In Fig. 4, the effect of sublaminate in-plane shear modulus G^s_{xy} on CSD in surface 90-plies of $[90_8/S_4]_s$ laminate is analyzed. FEM data and predictions of u_{1an} for different values of delamination length D_n at $\rho_n = 0.1$ and 0.5 are presented. The accuracy of fitting expressions is good over the whole range of used parameters. However, the accuracy decreases at large delamination length for $k = 0.5$.

However, when the u_{1an} expressions are used to predict the laminate shear modulus G^{LAM}_{xy} (equation (30) the results are in an excellent agreement with FEM values over the whole range of k, ρ_n and D_n (see Figs. 5 and 6). Even in the case $k = 0.5$ the agreement with FEM is excellent (a closer look reveals that the predicted is slightly lower than FEM, as expected with a too large u_{1an}).

5.2. Effect of ply thickness ratio

The effect of the sublaminate and the 90-ply thickness ratio was analyzed using cross-ply $[0_n/90_8]s$ and $[90_8/0_n]_s$ laminates. The predictive potential of expressions in Section 4 for u_{1an} in low and high crack density region can be evaluated comparing with FEM solutions as a function of the normalized delamination length D_n, see Fig. 7. The accuracy is very good over the whole range of used ply thicknesses, crack density and delamination length.

As expected from the above, the predicted laminate shear modulus (Figs. 8 and 9) at $\rho_n = 0.1$ and at $\rho_n = 0.5$ is in an excellent agreement with FEM.

6. Validation of the homogenization procedure for sublaminates

As shown is section 5, the accuracy of the shear modulus predictions using the GLOB-LOCdel expressions and fitting functions for CSD is very high for laminates with orthotropic sublaminates. In section 5 the sublaminate's stiffness elements were varied arbitrary, not thinking about the lay-up they may represent and the material. Some particular lay-ups are analyzed below.

First, we analyze the shear modulus dependence on crack density and local delamination length in GF/EP $[40_4/-40_4/90_8]_s$ laminate with UD elastic constants from [37] ($E_1 = 43GPa$, $E_2 = 13GPa$, $G_{12} = 4.69GPa$, $\nu_{12} = 0.3$ $G_{23} = 4.578GPa$ and $\nu_{23} = 0.42$). The $[40_4/-40_4]_s$ sublaminate's properties of relevance, calculated using CLT, are $G^s_{xy} = 12.16GPa$, $G^s_{yz} = 4.62GPa$. The rest of the sublaminate constants do not affect the shear response. The $[S_8/80_8]_s$ laminate's shear modulus (where $S = [40_4/-40_4]_s$) calculated using FEM and the GLOB-LOCdel expressions is shown in Fig. 10a for $\rho_n = 0.2$ and $\rho_n = 0.4$.

Next, the same homogenization procedure is applied to CF/EP $[0_8/45_4/-45_4/90_8]_s$ introducing sublaminate S=$[0_8/45_4/-45_4]_s$. The ply properties of the AS4-3502 CF/EP composite are taken from [38]: $E_1 = 144.8$ GPa, $E_2 = E_3 = 9.58$ GPa, $G_{LT} = 4.79$ GPa, $G_{T3} = 3.42$ GPa, $\nu_{12} = 0.31$, $\nu_{23} = 0.4$, leading to $G^s_{xy} = 21.07GPa$, $G^s_{yz} = 3.733GPa$. The FEM results and the GLOB-LOCdel predictions for the $[S_{16}/90_8]_s$ are shown in Fig. 10a and for both materials and lay-ups they are in good agreement.

Table 1
Values of parameter z_1/d for laminates used in parametric analysis.

Lay-up	$[S_4/90_8]_s[90_8/S_4]_s$	$[S_8/90_8]_s[90_8/S_8]_s$	$[S_{16}/90_8]_s[90_8/S_{16}]_s$
z_1/d	0.5	1.0	1.64

Calculations show that for all laminates with crack density $\rho_n = 0.1$ and $D_n = 0$ the cracks are non-interactive, $\varphi = 1$.

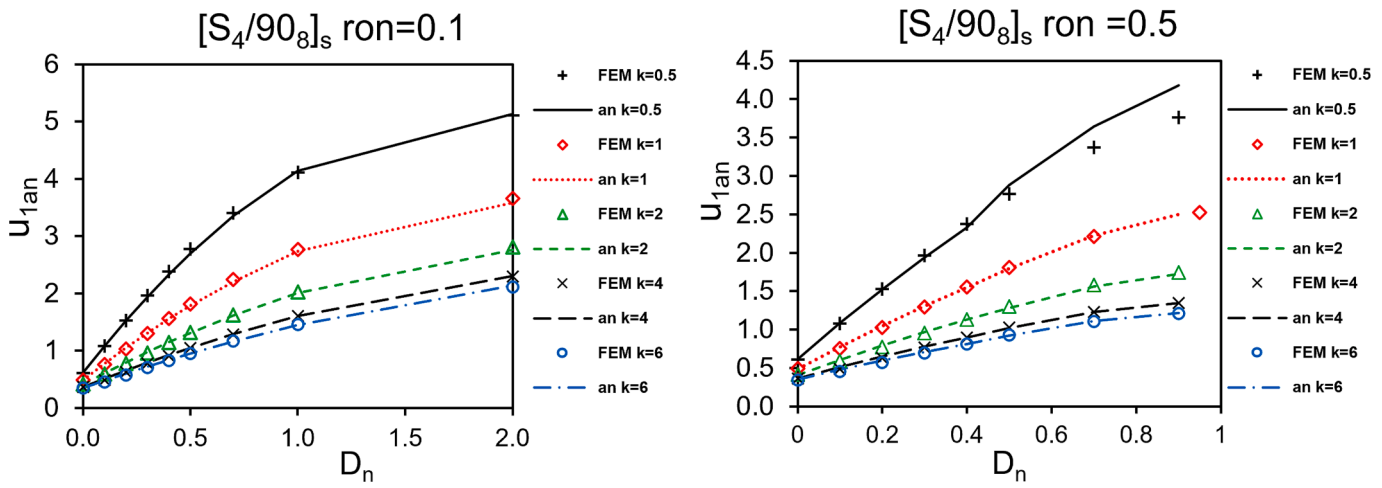

Fig. 3. Effect of sublaminate in-plane shear modulus $k = G^s_{xy}/G_{LT}$ on u_{1an} dependence on D_n in $[S_4/90_8]_s$ laminate at $\rho_n = 0.1$ and 0.5. FEM data are shown as symbols, simulations as lines.

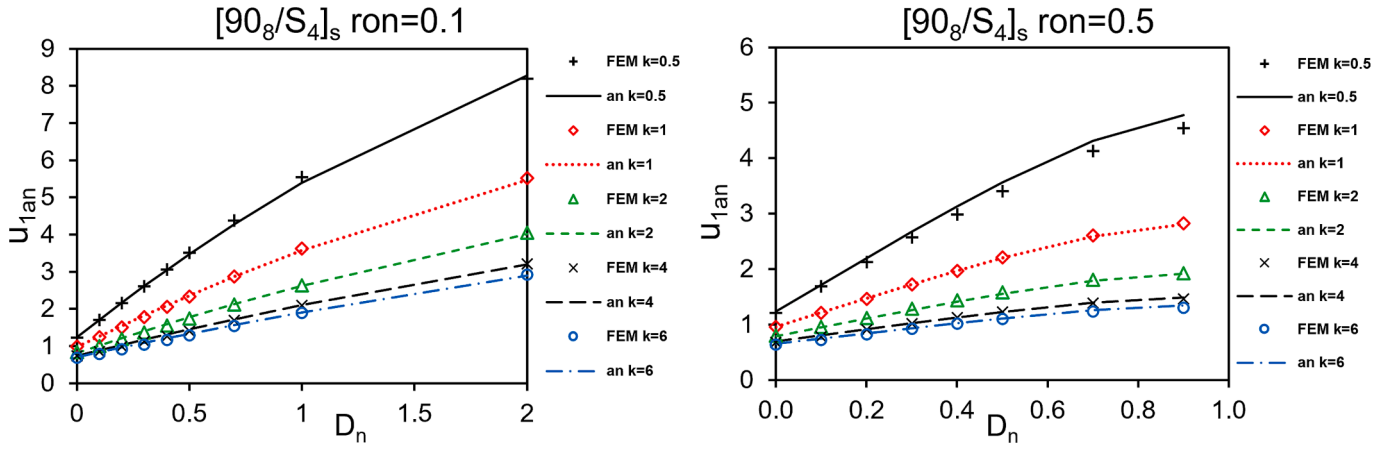

Fig. 4. Effect of sublaminate in-plane shear modulus G^s_{xy}/G_{12} on u_{1an} dependence on D_n in $[90_8/S_4]_s$ laminate at $\rho_n = 0.1$ and 0.5. FEM data are shown as symbols, calculations using expressions in section 4 as lines.

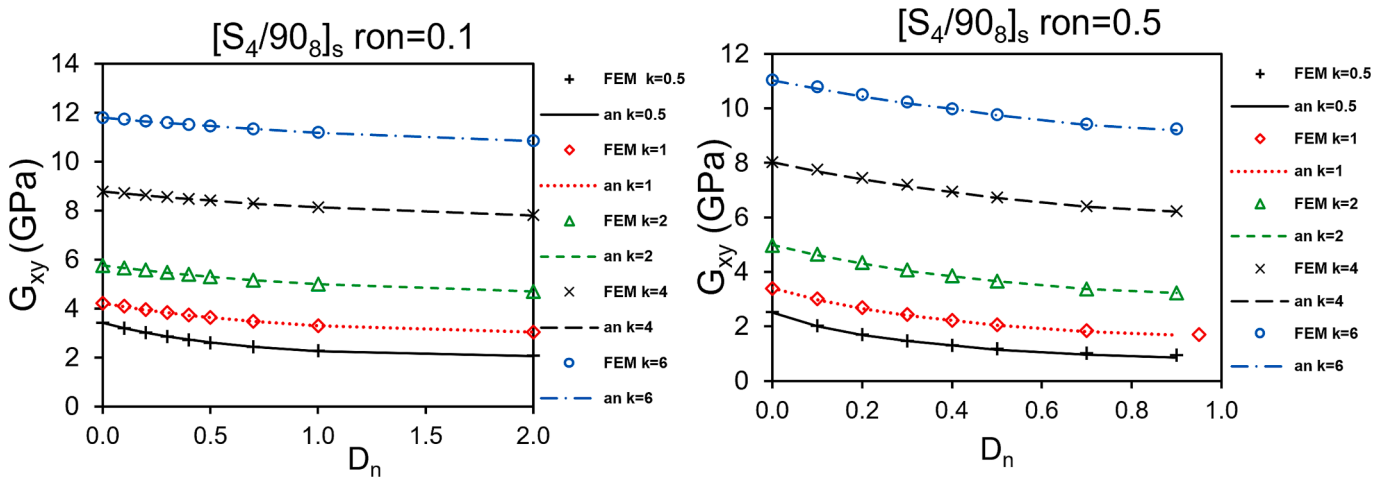

Fig. 5. Effect of sublaminate in-plane shear modulus on laminate shear modulus G^{LAM}_{xy}. Dependence on D_n in $[S_4/90_8]_s$ laminate is shown at $\rho_n = 0.1$ and 0.5. FEM data are shown as symbols, predictions using u_{1an} are shown as lines.

The homogenization path in the case of the CF/EP $[0_8/45_4/-45_4/90_8]_s$ laminate is not unique. The sublaminate S in the above calculation was introduced by homogenizing over the all plies (0,-45 and −45) surrounding the 90-ply. An alternative is a partial homogenization introducing a sublaminate with lay-up $S_0 = [45_4/-45_4]_s$ and analyzing stiffness change in $[0_8/S_{0\_8}/90_8]_s$ laminate. FEM calcu-

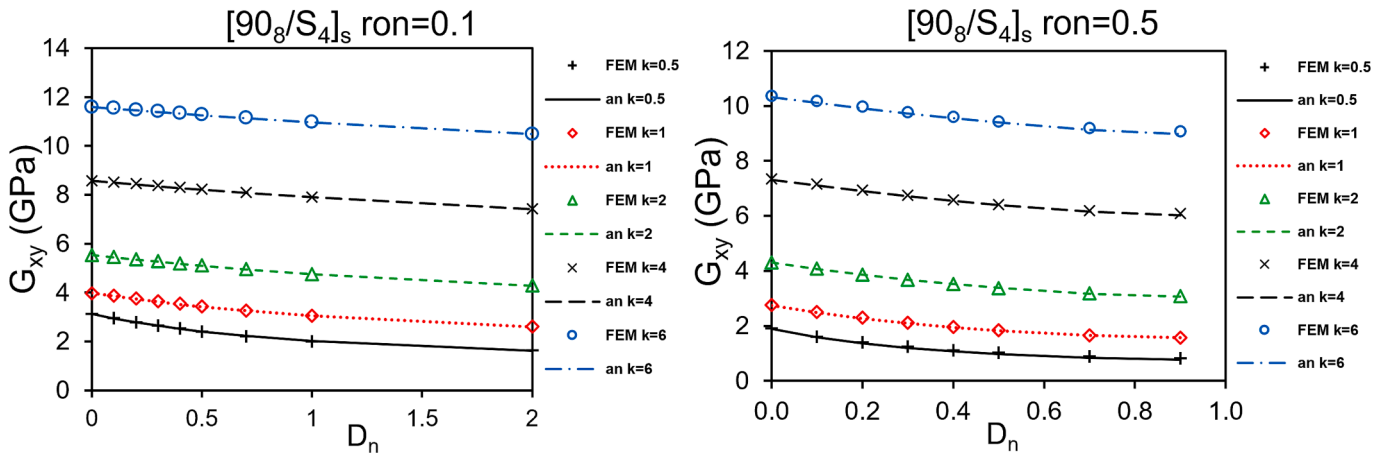

Fig. 6. Effect of sublaminate in-plane shear modulus on laminate shear modulus G_{xy}^{LAM}. Dependence on D_n for $[90_8/S_4]_s$ laminate is shown at $\rho_n = 0.1$ and 0.5. FEM data are shown as symbols, predictions using u_{1an} are shown as lines.

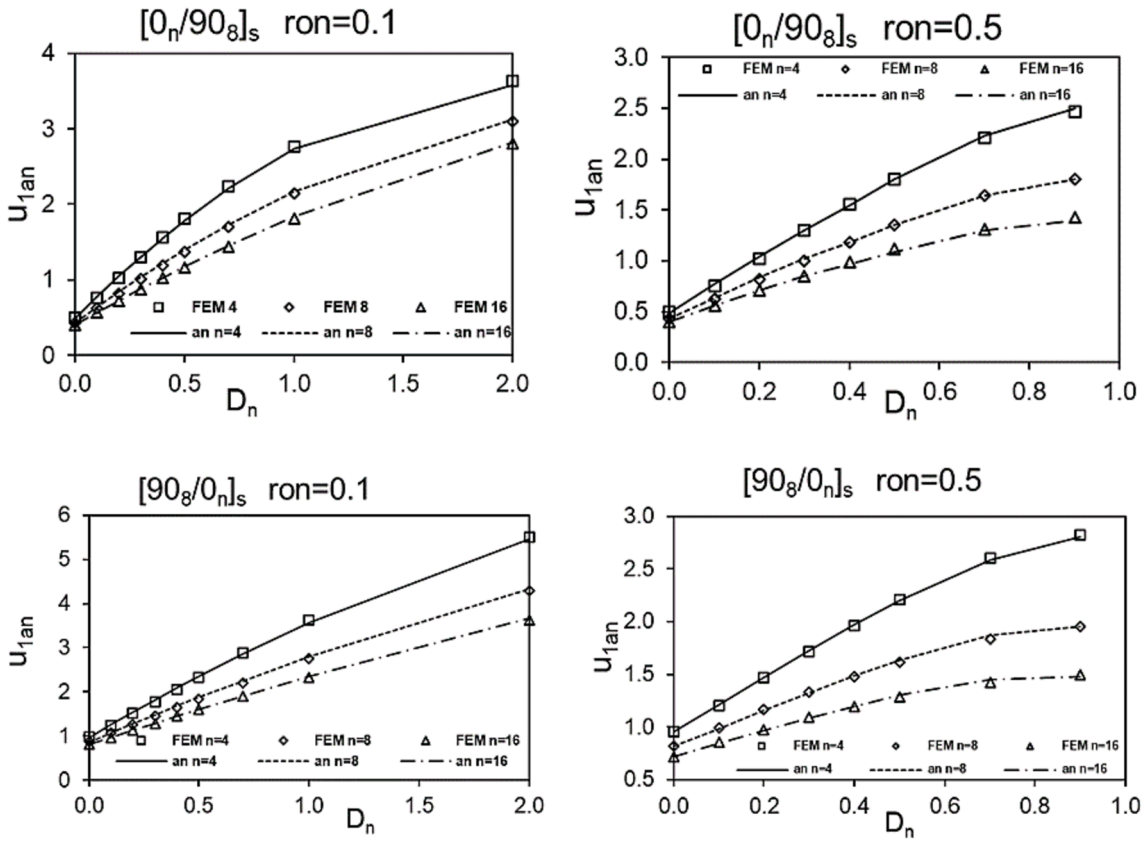

Fig. 7. Calculated sublaminate thickness effect on u_{1an}. Dependence on D_n is shown for $[0_n/90_8]_s$ and $[90_8/0_n]_s$ laminates at $\rho_n = 0.1$ and $\rho_n = 0.5$. FEM data are shown as symbols, curves with legends "an n = .." are predictions.

lations for both configurations (fully homogenized and partially homogenized support lay-up) are shown in Fig. 10b. The results are almost coinciding. This is a very important result showing that the shear modulus reduction is insensitive with respect to choices made regarding the lay-up for homogenization. It must be reminded that a homogenization leading to orthotropic sublaminate is benefiting the boundary condition formulation in FEM and that the fitting functions for CSD were obtained analyzing orthotropic sublaminates. A contributing factor to the robustness regarding the sublaminate selection is the used lay-up. The shear modulus of S_0 is much higher than for the rest of layers and it is understandable that the stiffness of the closest plies to the damaged have more effect on the CSD.

One could question the usefulness and the necessity of the homogenization. That may be true, but our own attempts to analyze damaged laminates with monoclinic layers and periodic boundary conditions using FEM inevitably resulted in artificial local stress concentrations at edges, concentrations that disappeared using orthotropic plies. In fact, the shear modulus of S_0 and the shear modulus of a 45 −ply in the global coordinates are similar and, therefore, the CSD for the homogenized and non-homogenized sublaminate case should be similar.

As a further validation of the used CSD expressions we compare our GLOB-LOCdel model with FEM calculations in [21] for shear modulus of

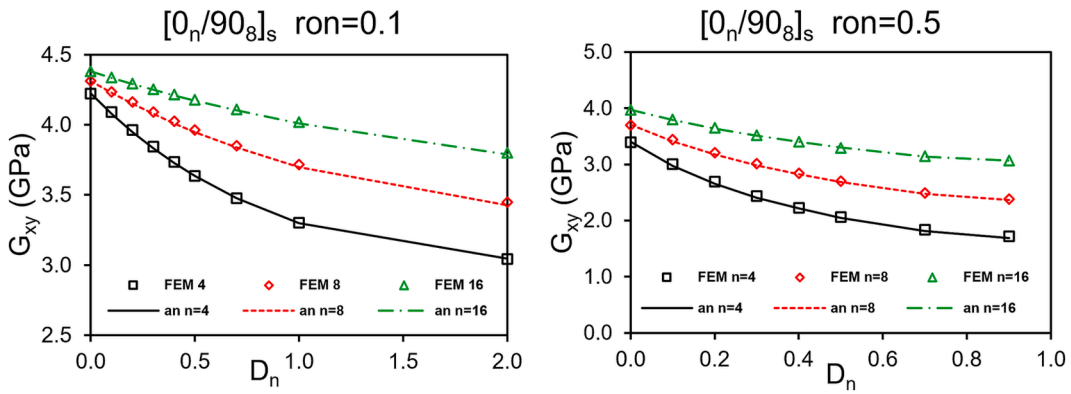

Fig. 8. Sublaminate thickness effect on laminate modulus G_{xy}^{LAM}. Dependence on D_n is shown for $[0_n/90_8]_s$ laminates at $\rho_n = 0.1$ and $\rho_n = 0.5$. FEM data are shown as symbols, curves with legends "an n=…" are predictions.

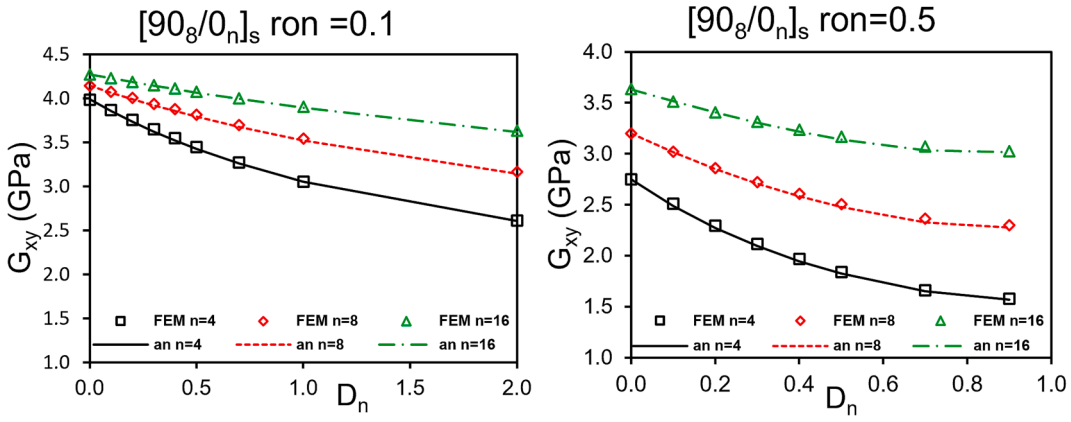

Fig. 9. Sublaminate thickness effect on laminate modulus G_{xy}^{LAM}. Dependence on D_n is shown for $[90_8/0_n]_s$ laminates at $\rho_n = 0.1$ and $\rho_n = 0.5$. FEM data are shown as symbols, curves with legends "an n=…" are predictions.

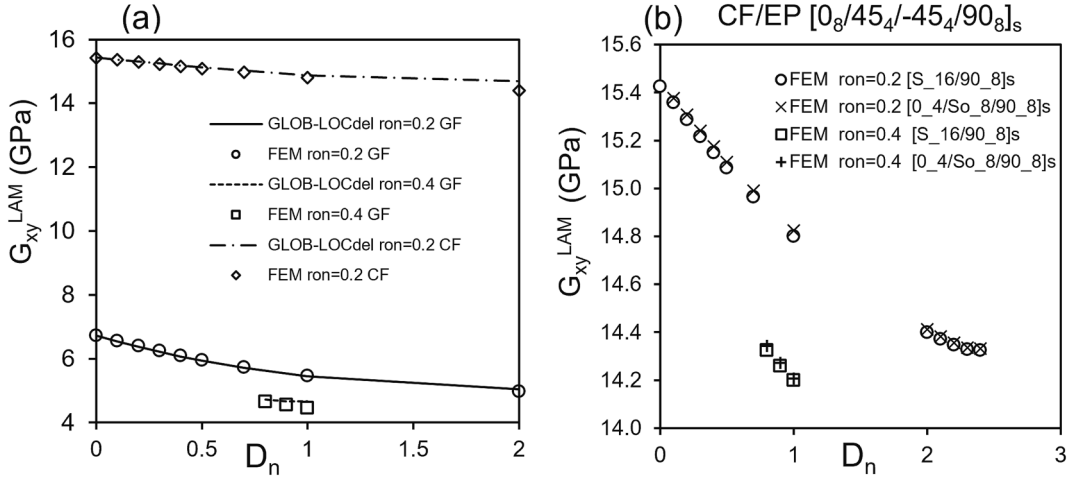

Fig. 10. Shear modulus G_{xy}^{LAM} of damaged GF/EP $[40_4/-40_4/90_8]_s$ and CF/EP $[0_8/45_4/-45_4/90_8]_s$ laminates as a function of normalized delamination length D_n at $\rho_n = 0.2$ and $\rho_n = 0.4$: a) FEM and GLOB-LOCdel results; b) FEM results for fully and partially homogenized sublaminates.

GFRP $[0/90_2/0/90_2]_s$ and $[0_2/45_2/-45_2/90_2]_s$ laminates. As shown in Fig. 11 agreement is excellent for both laminates in spite for rather extreme damage states (70 % of the interface is delaminated and the normalized crack density ρ_{90n} in $[0/90_2/0/90_2]s$ is rather high).

In Fig. 12 the GLOB-LOCdel results for laminate shear modulus are compared with the 2D shear lag model's predictions in [19]. This comparison is more to evaluate the shear model from [19] than our model which accuracy for a similar class of laminates has been shown above. Predictions of the model [19] in Fig. 12a are slightly lower that could be explained by the assumed zero stress in the delaminated region. However, the results in Fig. 12b are in a very good agreement except for the $\theta = 0$ case. It may be because the zero-stress assumption is more acceptable with larger delaminations and with higher shear modulus in global coordinates of the surrounding layers.

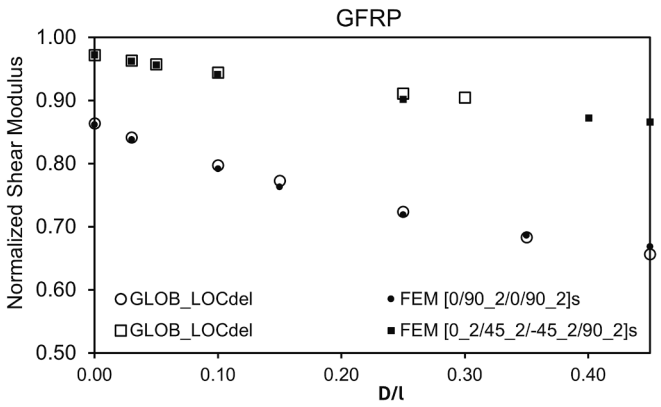

Fig. 11. Normalized in-plane shear modulus of GFRP laminates as a function of the relative delaminated area D/l: $[0/90_2/0/90_2]_s$ with $\rho_{90n} = 0.6$ and $[0_2/45_2/\text{-}45_2/90_2]_s$ with $\rho_{90n} = 0.3$. The ply properties are $E_1 = 48.8\text{GPa}, E_2 = 14.07\text{GPa}$ $G_{12} = 5.2\text{GPa}$, $\nu_{12} = 0.308, \nu_{23} = 0.4$. The GLOB-LOCdel predictions are shown as open symbols, FEM as closed symbols.

The GLOB-LOCdel simulation approach presented in this paper is aimed at predicting the thermo-elastic constants of laminates with known damage in plies (transverse cracks and local delaminations). However, experimental determination of the average delamination length is troublesome, since the delamination cracks are not open their observation and the length measurements are not reliable and possible only on the specimen edge where the stress state is 3D and delamination may be larger than inside of the specimen. Some data for cyclic loading of GFRP laminates are presented in [23]. The transverse crack density is relatively easy to measure using optical microscopy or x-ray CT.

This situation opens for a new application of the GLOB-LOCdel expressions: measuring the thermo-elastic constants of the damaged laminate and the crack density, the expressions can be used to estimate the average delamination length. That would bring valuable "experimental" information for validation of models simulating delamination growth in quasi-static and in cyclic loading.

7. Methodology for more complex cases

The GLOB-LOCdel expressions are applicable for all cases discussed below. However, the expressions for COD and CSD in section 4 are limited to the range of parameters and laminates used in FEM parametric analysis. The phenomena described below affect the COD and CSD values and in some cases, they have to be calculated differently than described in section 4. The suggestions apply for both COD and for CSD, but the magnitude of the effect can be different.

7.1. Nonuniform crack distribution and differences in delamination length

For a crack in a ply the distance to the adjacent crack on the left may be different than on the right. This affects the COD and CSD; the crack face that is closer to the adjacent crack will open and slide less. The analysis of the effect of the nonuniform distribution of cracks in the ply was presented in [39,40]. It was shown in [39] using FEM that assuming uniform crack distribution the laminate stiffness is slightly lower than for nonuniform. However, the difference becomes negligible if the nonuniformity coefficient $l_{min}/l_{av} > 0.7$.

Similarly, the delaminations for two cracks may have different length. This phenomenon was investigated in [21] showing numerically that the average delamination length for all cracks may be used with sufficient accuracy.

7.2. Nonsymmetric lay-up with respect to the damaged ply

Often the sublaminate S1 on the top of the damaged ply is different than S2 on the bottom. This feature affects the COD and CSD and it is not entirely clear how to calculate them. Suggestion was made in [1] that the top support sublaminate is mainly affecting the crack face displacements in the upper (top) part of the crack, whereas the bottom supporting sublaminate governs the opening and sliding of the lower part of the crack. Then, the normalized average crack opening and sliding displacement can be roughly estimated as an average of both effects. In case of $[S1/90_n/S2]$ this means that the average of COD and CSD in $[S1/90_n/S1]$ and $[S2/90_n/S2]$ has to be used.

7.3. Interaction with damage in other plies

Cracks in one damaged ply affect the COD and CSD in another damaged ply, especially if they are adjacent. This situation is not included in the CSD expressions presented in section 4 and mathematically more correct would using models were cracks in all plies are present and interacting. That would introduce a large number of parameters and derivation of fitting expressions would not be practically feasible. A method called by authors "Equivalent Constraint Model" was introduced in [19] and similar ideas were used in [29]. Analyzing the COD and CSD in one damaged ply the rest of plies is homogenized and analysis performed for sublaminates with effective stiffness.

The effective properties of a ply are found as described below. Start with assuming that only one of the plies with index k_1 has cracks and use the GLOB-LOCdel to calculate the stiffness matrix of the laminate $[Q]^{LAM}$. Then, calculate the effective stiffness of the damaged ply $[\overline{Q}]^{d}_{k_1}$ in global

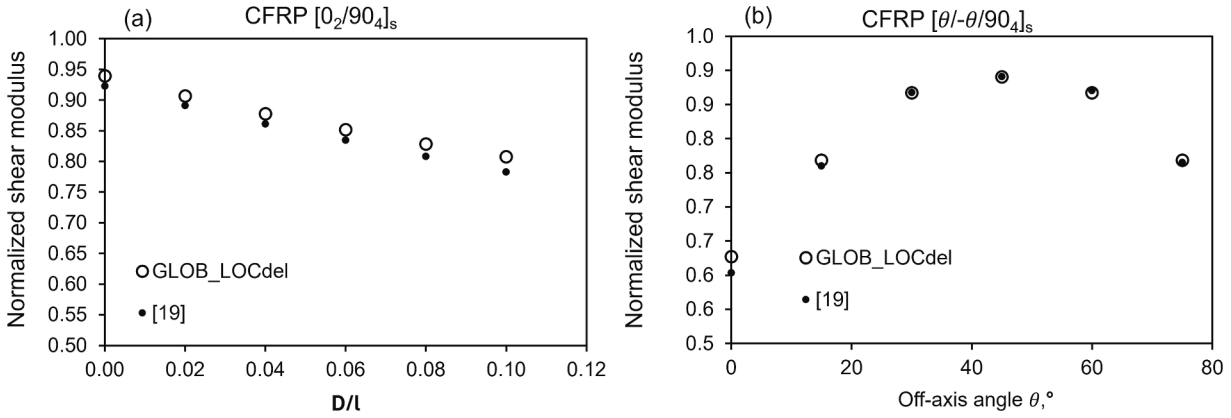

Fig. 12. Normalized shear modulus of CFRP laminate with cracks and delaminations. Predictions using the GLOB-LOCdel model are shown as open symbols, results from [19] are presented as closed symbols: a) dependence on the relative delaminated area for $\rho_{90n} = 0.1$; b) dependence on orientation angle θ for $\rho_{90n} = 0.25$ and $D_n = 2$. The UD ply elastic constants are $E_1 = 144.8\text{GPa}, E_2 = 11.38\text{GPa}$ $G_{12} = 6.48\text{GPa}$, $\nu_{12} = 0.3, G_{23} = 3.45$ GPa.

coordinates from the difference between the damaged and undamaged laminate stiffness

$$[\overline{Q}]^{d}_{k_1} = [\overline{Q}]_{k_1} - \frac{1}{t_{k_1}}\left\{[Q]^{LAM} - [Q]^{LAM}_{0}\right\} \quad (49)$$

Calculate the effective elastic constants of the damaged ply in local coordinates using stiffness transformation. This is repeated for all damaged plies.

In the next iteration, calculating the COD and CSD of cracks in the same ply, the effective stiffnesses of other plies must be used in expressions in section 4. The number of iterations is small, 5–8 iterations give more than sufficient accuracy [19,29]. However, the results in [29] indicate that the account of crack interactions in average by using effective stiffness may not be sufficient and the calculated CSD and COD are higher and the stiffness reduction lower than in FE models with explicit system of several crack types. It appears, that the effective stiffness can be efficiently used only for plies that are not the adjacent to the analyzed ply. Apart from that, the effect of interaction is different for different elastic constants. For example, the interaction effect of cracks in 90- and 0-ply in [0/90]s is negligible for the laminate axial modulus but very important for its shear modulus.

7.4. Application in bending problems

In applications when bending of the laminate takes place the approach with effective stiffness of the damaged plies, using it in the laminate theory, can be suggested. Its efficiency has been shown, for example, in [35]. However, in bending, cracks in some layers are closed and in a central ply the crack is partially closed. This means that the effective ply stiffness depends on the position of the damaged ply in the laminate. It seems safe to say that the effective stiffness can be used for plies that are thin comparing with the laminate thickness and far away from the midplane (the z-dependence of in-plane stresses in the ply is weak) and located in the tensile part of the laminate. In the compressive part of the laminate cracks are closed, COD = 0, and sliding displacement, ignoring friction, is the same as before.

8. Conclusions

A simulation tool (GLOB-LOCdel) with ability to predict the whole set of in-plane thermo-elastic constants of symmetric laminates with damage in plies is presented. Damage is represented by transverse crack density that is different in different plies and the average length of local delaminations radiating from the crack along the ply interface. Exact elasticity expressions are linking the laminate's macroscopic constants with the two above damage characteristics and the two characteristics of the crack: its opening (COD) and sliding (CSD) displacements. The COD and CSD are strongly affected by delamination length.

The COD and CSD define the in-plane elements of the Vakulenko-Kachanov tensor that is used in the formulation of the GLOB-LOCdel approach. The out-of-plane elements of the tensor that describe the out-of-plane stiffness are not analyzed, focusing on the in-plane response. The CSD dependence on crack density and delamination length is analyzed using the surrounding lay-up (ply orientations, thicknesses and elastic constats) as a parameter in FEM model and high accuracy approximation functions for CSD are presented. Validation examples for different balanced laminates show the robustness and the accuracy of the methodology that involves homogenization over the couples of monoclinic plies.

The GLOB-LOCdel model can also be used to solve the inverse problem of determining the average local delamination length (not easy observable and quantified) by measuring the axial modulus and the crack density.

CRediT authorship contribution statement

Janis Varna: Writing – review & editing, Writing – original draft, Visualization, Validation, Supervision, Methodology, Investigation, Formal analysis, Data curation. **Rodrigo T.S. Freire:** Writing – review & editing, Validation, Formal analysis, Data curation, Conceptualization. **Mohamed Sahbi Loukil:** Writing – review & editing, Validation, Supervision, Methodology, Investigation, Data curation. **Nawres J. Al-Ramahi:** Data curation.

Declaration of competing interest

The authors declare that they have no known competing financial interests or personal relationships that could have appeared to influence the work reported in this paper.

Data availability

Data will be made available on request.

References

[1] Varna J. Modeling mechanical performance of damaged laminates. J Compos Mater 2013;47(20–21):2443–74.
[2] Parvizi A, Bailey JE. On multiple transverse cracking in glass fibre epoxy cross-ply laminates. J Mater Sci 1978;13:2131–6.
[3] Jamison RD, Schulte K, Reifsnider KL, Stinchcomb WW. Characterization and analysis of damage mechanisms in tension-tension fatigue of Graphite/Epoxy laminates. ASTM STP 1984;836:21–55.
[4] Joffe R, Varna J. Analytical modeling of stiffness reduction in symmetric and balanced laminates due to cracks in 90° layers. Compos Sci Technol 1999;59:1641–52.
[5] Kashtalyan M, Soutis C. Analysis of composite laminates with intra- and interlaminar damage. Prog Aerosp Sci 2005;41:152–73.
[6] Takeda N, Ogihara S, Kobayashi A. Microscopic fatigue damage progress in CFRP cross-ply laminates. Composites 1995;26:859–67.
[7] Varna J. Strategies for stiffness analysis of laminates with microdamage: combining average stress and crack face displacement based methods, ZAMM · Z. Angew Math Mech 2015;95(10):1081–97.
[8] Nairn, J. and Hu, S. (1994), Matrix microcracking, in: Pipes, R.B., Talreja, R. eds. Damage Mechanics of Composite Materials. Composite Materials series, vol. 9, Elsevier, Amsterdam, 187-243.
[9] Smith PA, Wood JR. Poisson's ratio as a damage parameter in the static tensile loading of simple cross-ply laminates. Compos Sci Technol 1990;38:85–93.
[10] Hashin Z. Analysis of cracked laminates: a variational approach. Mech of Mater, North-Holland 1985;4:121–36.
[11] Varna J, Berglund LA. Multiple Transverse Cracking and Stiffness Reduction in Cross-Ply Laminates. J Compos Technol Res, JCTRER 1991;13(2):97–106.
[12] Varna J, Berglund LA. Thermo-elastic properties of composite laminates with transverse cracks. J Compos Technol Res 1994;16(1):77–87.
[13] Zhang J, Fan J, Soutis C. Analysis of multiple matrix cracking in [±θm/90n]s composite laminates. Part 1. In-plane stiffness properties. Composites 1992;23(5):291–304.
[14] McCartney LN, Schoeppner GA. Predicting the effect of non-uniform ply cracking on the thermo-elastic properties of cross-ply laminates. Compos Sci Technol 2000;62:1841–56.
[15] McCartney LN, Schoeppner GA, Becker W. Comparison of models for transverse ply cracks in composite laminates. Comp Sci Technol 2000;60:2347–59.
[16] Hajikazemi M, McCartney NL. Comparison of variational and generalized plane strain approaches for matrix cracking in general symmetric laminates. Int J Damage Mechanics 2016.
[17] O'Brien, T.K. (1982) Characterization of delamination onset and growth in a composite laminate. Damage Compos. Mater. Basic Mech. Accumulation, Toler. Charact. 140–167.
[18] McCartney LN, Blazquez A, Paris F. Energy-based delamination theory for biaxial loading in the presence of thermal stresses. Compos Sci Technol 2012;72(14):1753–66.
[19] Kashtalyan M, Soutis C. The effect of delaminations induced by transverse cracks and splits on stiffness properties of composite laminates. Compos Part A 2000;31:107–19.
[20] Kashtalyan M, Soutis C. Analysis of local delaminations in composite laminates with angle-ply matrix cracks. Int J Solids Struct 2002;39:1515–37.
[21] Carraro PA, Maragoni L, Quaresimin M. Stiffness degradation of symmetric laminates with off-axis cracks and delamination: an analytical model. Int J Solids Struct 2021;213:50–62.
[22] Hajikazemi M, Ahmadi H, McCartney LN, Van Paepegem W. A variational approach for accurate prediction of stress and displacement fields and thermo-elastic constants in general symmetric laminates containing ply cracking and

delamination under general triaxial loading. Int J Solids Struct 2022;254–255:111917.
[23] Maragoni L, Carraro PA, Simonetto M, Quaresimin M. A novel method to include crack-induced delamination in a fatigue damage predictive procedure for composite laminates. Compos Sci Technol 2023;238:110011.
[24] Gudmundson P, Östlund S. First order analysis of stiffness reduction due to matrix cracking. J Comp Mater 1992;26:1009–30.
[25] Gudmundson P, Zang W. A universal model for thermoelastic properties of macro cracked composite laminates. Int J Sol Struct 1993;30:3211–31.
[26] Lundmark P, Varna J. Modeling thermo-mechanical properties of damaged laminates. Key Eng Mater 2003;251–252:381–7.
[27] Lundmark P, Varna J. Constitutive relationships for damaged laminate in in-plane loading. Int J Dam Mech 2005;14(3):235–59.
[28] Joffe R, Krasnikovs A, Varna J. COD-based simulation of transverse cracking and stiffness reduction in [S/90n]s laminates. Comp Sci Technol 2001;61:637–56.
[29] Lundmark P, Varna J. Crack face sliding effect on stiffness of laminates with ply cracks. Comp Sci Technol 2006;66:1444–54.
[30] Lundmark P, Varna J. Stiffness reduction in laminates at high intralaminar crack density: effect of crack interaction. Int J Damage Mech 2011;20(2):279–97.
[31] Loukil MS, Varna J, Ayadi Z. Engineering expressions for thermo-elastic constants of laminates with high density of transverse cracks. Composites A 2013;48(1):37–46.
[32] Loukil MS, Varna J. Crack face sliding displacement (CSD) as an input in exact GLOB-LOC expressions for in-plane elastic constants of symmetric damaged laminates. Int J Damage Mech 2020;29(4):547–69.
[33] Allen DH, Yoon C. Homogenization techniques for thermo-viscoelastic solids containing cracks. Int J Solids Struct 1998;35:4035–53.
[34] Varna J, Loukil MS. Effective transverse modulus of a damaged layer: Potential for predicting symmetric laminate stiffness degradation. J Compos Mater 2017;51(14):1945–59.
[35] Pupurs A, Varna J, Loukil M, Ben Kahla H, Mattsson D. Effective stiffness concept in bending modeling of laminates with damage in surface 90-layers. Compos A 2016;82(22):244–52.
[36] Giannadakis K, Varna J. Potential of a simple variational analysis in predicting shear modulus of laminates with cracks in 90-layers. J Compos Mater 2014;48(15):1843–56.
[37] Katerelos DG, Kashtalyan M, Soutis C, Galiotis C. Matrix cracking in polymeric composites laminates: Modelling and experiments. Compos Sci Technol 2008;68(12):2310–7.
[38] Groves SE, Harris CE, Highsmith AL, Allen DH, Norvell RG. An experimental and analytical treatment of matrix cracking in cross-ply laminates. Exp Mech 1987;27:73–9.
[39] Loukil MS, Varna J, Ayadi Z. Applicability of solutions for periodic intralaminar crack distributions to non-uniformly damaged laminates. J Compos Mater 2013;47(3):287–301.
[40] McCartney LN, Schoeppner GA. Predicting the effect of non-uniform ply cracking on the thermo-elastic properties of cross-ply laminates. Compos Sci Technol 2000;62:1841–56.